CO2 loss by permafrost thawing implies additional emissions reductions to limit warming to 1.5 or 2 °C

CO_2 loss by permafrost thawing implies additional emissions reductions to limit warming to 1.5 or 2 °C

Eleanor J. Burke[1], Sarah E. Chadburn[2], Chris Huntingford[3] and Chris D. Jones[1]

[1]Met Office Hadley Centre, FitzRoy Road, Exeter, EX1 3PB, UK
[2]University of Leeds, School of Earth and Environment, Leeds, LS2 9JT, UK
[3]Centre for Ecology and Hydrology, Wallingford, Oxfordshire, OX10 8BB, U.K.

Abstract

Large amounts of carbon are stored in the permafrost of the northern high latitude land. As permafrost degrades under a warming climate, some of this carbon will decompose and be released to the atmosphere. This positive climate-carbon feedback will reduce the natural carbon sinks and thus lower anthropogenic CO_2 emissions compatible with the goals of the Paris Agreement. Simulations using an ensemble of the JULES-IMOGEN intermediate complexity climate model (including climate response and process uncertainty) and a stabilization target of 2 °C, show that including the permafrost carbon pool in the model increases the land carbon emissions at stabilization by between 0.09 and 0.19 Gt C year^{-1} (10th to 90th percentile). These emissions are only slightly reduced to between 0.08 and 0.16 Gt C year^{-1} (10th to 90th percentile) when considering 1.5 °C stabilization targets. This suggests that uncertainties caused by the differences in stabilization target are small compared with those associated with model parameterisation uncertainty. Inertia means that permafrost carbon loss may continue for many years after anthropogenic emissions have stabilized. Simulations suggest that between 225 and 345 Gt C (10th to 90th percentile) are in thawed permafrost and may eventually be released to the atmosphere for stabilization target of 2 °C. This value is 60 to 100 Gt C less for a 1.5 °C target. The inclusion of permafrost carbon will add to the demands on negative emission technologies which are already present in most low emissions scenarios.

Introduction

Northern high latitude permafrost soils contain large amounts of relatively inert soil carbon (Hugelius et al., 2014). Under increased temperatures associated with anthropogenic burning of fossil fuels, permafrost will degrade and a proportion of the old inert carbon present will become vulnerable to decomposition. This will cause a release of carbon dioxide (CO_2) into the climate system. This process is irreversible on human timescales (i.e. centuries), and so will result in a further increase in greenhouse gases in the atmosphere. Hence this is a positive carbon climate feedback, adding to the effects of anthropogenic emissions through fossil fuel burning (Schuur et al., 2015; MacDougall et al., 2012; Schneider von Deimling et al., 2015; Burke et al., 2012; 2013; 2017b). Recent papers suggest that the permafrost carbon feedback to climate change will be, in relative terms, a more important climate change feedback in scenarios with substantial mitigation (Burke et al., 2017b; MacDougall et al, 2012; González-Eguino and Neumann, 2016). Burke et al. (2017b) carried out a systematic uncertainty analysis of this feedback and showed the additional warming from the permafrost carbon feedback under the RCP2.6 strong mitigation scenario is between 4 and 18 % of the change in the global mean temperature (ΔT). This range reflects differences in land surface models and climate response.

The agreement at the year 2015 United Nations Framework Convention on Climate Change (UNFCCC) Conference Of Parties (COP) meeting in Paris was to commit to keeping global temperature rise below 2 °C since pre-industrial times, while pursuing efforts to limit temperature increase to 1.5 °C (Schleussner et al., 2016; Rogelj et al., 2015). The pathways that are consistent with these targets typically require major reductions in emissions, and even large amounts of deliberate CO_2 removal from the atmosphere. Negative emissions technologies (NETs) are therefore present in the majority of low emissions scenarios (Smith et al., 2016) and used to offset any remaining emissions from fossil fuels and land use change. Currently natural land and ocean carbon sinks together absorb approximately half of the anthropogenic CO_2 emissions (Jones et al., 2016). Earth system models (ESMs) suggest a significant weakening of these sinks can be expected in to the future, even under a low emissions scenario (Jones et al., 2016). Any modification of the natural carbon cycle in response to climate change will impact the global emission pathways to achieve climate stabilisation. In the event of positive feedbacks, it may increase the need for NETs.

We hypothesise that permafrost carbon release will require extra mitigation effort to achieve either a 1.5 °C or 2 °C stabilization target. This hypothesis is tested and the extra mitigation quantified using a climate modelling system of intermediate complexity coupled with a new generation process-oriented land surface model that includes permafrost processes. Additionally we quantify uncertainties in the permafrost carbon release resulting from uncertainties in climate change projections and the parameterisation of the soil carbon decomposition.

Materials and Methods

JULES land surface scheme

This analysis is based on a version of the Joint UK Land Environment Simulator (JULES - Best et al., 2011; Clark et al., 2011). This is the land surface component of the UK Earth System Model (UKESM - Jones and Sellar, 2016), and our permafrost-adapted version of JULES (v4.3) is described in Chadburn et al. (2015a) and Burke et al. (2017a). JULES describes the physical, biophysical and biochemical processes that control the exchange of radiation, momentum, heat, water and carbon between the land surface and the atmosphere. It can be applied at a point or over a grid, and requires temporally continuous meteorological forcing data at sub-daily timesteps (air temperature, humidity, longwave and shortwave incoming radiation, precipitation, wind speed and air pressure) along with atmospheric CO_2 concentration. JULES simulates the terrestrial response to changes in these climate data. Each point or grid box can be divided up into several different (non-spatially explicit) land-cover types. These include five different plant functional types (broadleaf trees, evergreen trees, C_3 and C_4 grasses and shrubs) plus non-vegetated land-cover (urban, water, ice and bare soil). The fraction of each land-cover type within a grid box is used to calculate the surface energy balance, but the soil underneath is treated as a single column and receives aggregated mean fluxes from the surface. JULES includes a dynamic vegetation model which simulates the vegetation distribution and its response to climate change (Clark et al., 2011).

Several important modifications have been added into JULES to improve the representation of physical and biogeochemical processes in the cold regions. New modelled physical processes

include the additional impact of the insulation effects of a moss layer at the soil surface. Updated soil thermal and hydraulic properties now take account of the presence of organic matter. JULES can have a deeper and better resolved soil column and an additional thermal column at the base of the soil to represent bedrock (Chadburn et al., 2015a; 2015b). In this work JULES has 16 soil layers which increase in thickness from 5 cm at the surface to 5 m for the deepest model level (total soil depth is 18.3 m). Below this model level there is bedrock in which only thermal processes are simulated. Burke et al. (2017a) introduced a vertically resolved soil carbon decomposition model which uses the same discretisation as the soil physics - although the parameterisation of mixing processes means there is minimal soil carbon below 3 m. This model now enables the 'old' soil carbon within the permanently frozen soil to be identified at the start of the simulation and traced throughout the simulation, including its fate in a warming world. The contribution of this 'old' soil carbon to the land-atmospheric CO_2 flux can be excluded in our modelling framework. It should be noted that JULES simulates an on-going small exchange between the carbon above and below the permafrost table. This is caused by mixing processes and very slow simulated decomposition in the permafrost. This means that in the model and over very many thousands of years all the old carbon in the permafrost will eventually turn over and be replaced by carbon from above the permafrost table.

Uncertainty in the parameterisation of the soil carbon decomposition model is incorporated through two different responses to temperature. Each response has its own e-folding depth through which respiration (i.e. release of CO_2 back to the atmosphere) becomes lower as depth increases (Burke et al., 2017a). These are denoted JULES-suppressR_{esp} and JULES-deepR_{esp} (Burke et al., 2017b). JULES-suppressR_{esp} uses an Arrhenius function with Q_{10}=2.0 and has more suppressed respiration with depth and a greater proportion of its respiration from nearer the surface. JULES-deepR_{esp} uses the temperature dependence from the Roth C soil carbon model (Jenkinson, 1990; Clark et al., 2011) and has a greater proportion of its respiration from deeper in the soil. In both parameterisations, the summer peak of the present-day soil respiration is very similar (Burke et al., 2017b). Further work constraining the model with additional observational data is required to rule out one or other of the parameterisations.

IMOGEN

The Integrated Model Of Global Effects of climatic aNomalies (IMOGEN) is an intermediate complexity climate model. IMOGEN contains a simple energy balance model (EBM; Huntingford and Cox, 2000) that relates changes in concentrations of atmospheric greenhouse gases to the global mean land temperature response via changes in a radiative forcing. It uses a "pattern-scaling" approach to then relate, linearly, the amount of annual global average warming over land to monthly changes in local meteorology. This local meteorology is disaggregated to hourly timesteps, and then used to drive the JULES model. The global land-atmosphere carbon flux from JULES (which can include 'old' soil carbon fluxes) is returned to IMOGEN and used within IMOGEN to adjust atmospheric CO2 concentration, and thus the radiative forcing. The land-ocean CO2 flux is calculated using a single "box" model, and is a function of global temperature increase and atmospheric CO2 level (Huntingford et al., 2004). As IMOGEN has both land- and ocean-atmosphere feedbacks, then it can be forced with anthropogenic CO2 emissions which determine evolving atmospheric CO2 concentration. IMOGEN is calibrated to emulate the 22 different GCMs described in Zelazowski et al. (2016), and provides a full range of climate responses.

Experimental design and evaluation methods

Burke et al. (2017b) set out the initial modelling framework which we have extended to determine the emissions compatible with a climate stabilisation at either 1.5 or 2.0 °C and used to quantify the impact of the permafrost CO_2 feedback on the global carbon cycle. Uncertainties include those from the driving GCMs and two alternative land surface parameterisations describing the northern high latitude terrestrial cryosphere response.

The coupled JULES-IMOGEN model was first "spun-up" using pre-industrial atmospheric CO_2 and the 1961-1990 Water and Global Change forcing data (Weedon et al., 2011) so that it has stable soil carbon and vegetation distributions approximately representative of pre-industrial conditions. This was performed separately using both the JULES-suppressR_{esp} and JULES-deepR_{esp} representations of soil carbon and its respiration. The initialisation and spin-up protocol is described in further detail in Burke et al. (2017b). These global spun-up states were then used to initialize an ensemble of transient simulations starting in 1860, describing the

effects of historical climate change, followed by future scenarios for the available range of climate responses (Zelazowski et al., 2016). The historical simulations were forced with known historical fossil fuel and cement production CO_2 emissions. These were then followed using the emissions representing the RCP8.5 Representative Concentration Pathway used in the fifth assessment report of the Intergovernmental Panel on Climate Change (IPCC, 2013; Moss et al., 2010). At a specified year, depending on the climate response and the global mean temperature target for stabilization, the anthropogenic emissions were reduced to zero. This year was defined such that the simulations have a global mean temperature change of 1.5 or 2 °C ± 0.05 °C between 1860 and 2500. For the rest of the simulation the land- and ocean- atmosphere fluxes are balanced by compatible emissions so that the net emissions remain at zero and the radiative forcing and hence atmospheric CO_2 concentration remains fixed.

To isolate the feedback associated with permafrost CO_2 release due to thawing we identified the permafrost carbon representative of pre-industrial times. Permafrost carbon (and permafrost) is assumed to exist at any depths where the soil is continually frozen during the first two years of the simulation. An additional ensemble was run without the atmospheric response to any emissions from this permafrost carbon. Therefore, for each ensemble member, there are paired simulations available where the difference in the global mean temperature within each pair is an estimate of the permafrost CO_2 feedback (Burke et al., 2017b). There are four sub-ensembles: JULES-suppressR_{esp} with a 1.5 °C target; JULES-deepR_{esp} and 1.5 °C; JULES-suppressR_{esp} and 2 °C; JULES-deepR_{esp} and 2 °C. Each of these sub-ensembles contains 22 estimates of the permafrost carbon feedback which encompass the range of climate responses of the calibration GCMs. These feedback estimates were used to define cumulative distributions of the permafrost CO_2 feedback for each sub-ensemble. These represent the fraction of the ensemble members with a feedback less than the value shown. Additional emissions which have not been included in this framework from, for example, non-CO_2 greenhouse gases, aerosols and land use change will have a minor impact on the permafrost CO_2 feedback.

Burke et al. (2017b) assessed in detail the present day states of both JULES-suppressR_{esp} and JULES-deepR_{esp}. Here we highlight two of the most relevant comparisons - with the Brown et al. (1998) map of permafrost extent and with an approximate estimate of the permafrost carbon derived from the Northern Circumpolar Soil Carbon Database version 2 observations (NCSCDv2; Hugelius et al., 2014) dataset. The low resolution of the model simulations means

that the modelled and observed permafrost extents are not exactly comparable. However, the simulated extent might be expected to fall within the area encompassed by continuous plus discontinuous permafrost (~15.7 million km^2) and sporadic, continuous and discontinuous permafrost (~19.6 million km^2). In order to quantify the observed permafrost carbon we additionally require a spatially distributed estimate of the top of the permafrost table. Since this is unavailable we assume that it tends to fall somewhere from 0.3 to 1.0 m for the majority of the permafrost. This gives a range of estimates of the carbon in the permafrost. The climate response of IMOGEN was assessed by comparing the relationship between the cumulative anthropogenic carbon emissions and the global mean air temperature change with that derived from the model simulations used in IPCC (2013).

Results

Assessment of model simulations

The modelling framework is structured so that the simulated time series of the global mean temperature stabilises by 2500 at either 1.5 or 2 °C above that of 1860 (Figure 1a). By the end of the 21st century the global mean temperature has increased to a value only slightly less than the stabilization target. It then slowly approaches the prescribed target over the next 400 years. The spread of values depicted reflects the different climate responses of the individual GCMs emulated by the IMOGEN system. The relationship between the cumulative anthropogenic surface emissions and the surface air temperature increase (Supplementary information - Figure 1) falls within the spread shown in the IPCC (2013) report for the CO_2 only case. In addition, the historical time series of global soil, vegetation and land carbon change are comparable with those found in Jones et al (2013) without land use (Supplementary information - Figure 2).

Figure 1b shows the permafrost physics and its response to the changing climate. The mean simulated permafrost extent between 1960 and 1990 is between 16.6 and 17.1 million km^2. The model captures all of the observed continuous permafrost (Brown et al., 1998 – defined as more than 90 % of a grid cell underlain by permafrost) but has slightly too much discontinuous permafrost, particularly in Eurasia (Supplementary information - Figure 3). Therefore, it slightly over estimates the observed area of continuous plus discontinuous permafrost (15 million km^2). However, in general terms, we consider that JULES can describe the permafrost state of the

recent past (see Burke et al., 2017b for further details). Over the 20th century the model simulates a slow loss of permafrost of around 0.05 million km^2 per decade. This loss accelerates during the 21st century to between 0.15 and 0.26 million km^2 per decade for the 2 °C pathway. Eventually the loss slows down towards the end of the 21st century – more so for the for the 1.5 °C pathway than the 2 °C pathway. The slightly longer timescales associated with the soil physics compared to the global mean temperature implies that after year 2100, the permafrost takes up to an additional 40 or so years to stabilise whereas the global mean temperature is relatively stable (Figure 1a). Our modelling system estimates that the final remaining extent is between 13.5 and 14.5 million km^2 for 2 °C stabilization - a loss of between 2.5 and 3.5 million km^2 since pre-industrial. Under the 1.5 °C target and by 2500 the permafrost area is on average 0.7 million km^2 larger than under the 2 °C target. In addition, the top of the permafrost table is around 0.3 m deeper at 1.5 °C stabilization and 0.55 m deeper at 2 °C stabilization, when compared to pre-industrial conditions.

JULES-suppressR_{esp} and JULES-deepR_{esp} have different initial soil carbon distributions with JULES-deepR_{esp} having more soil carbon both in the northern high latitudes and the permafrost (Figure 1c, 1d). This is caused by JULES-deepR_{esp} having less soil respiration at temperatures below zero (See Figure 1 of Burke et al., 2017a). Although there are differences between the amount of permafrost carbon in JULES-suppressR_{esp} and JULES-deepR_{esp}, they both fall within the range of plausible values derived from the NCSCDv2 observations (Figure 1c, 1d).
Any loss of permafrost and the associated increase in maximum annual active layer thickness will result in less soil carbon within the permafrost (Figure 1c and 1d). The soil carbon just below the maximum active layer thickness in year 1900 will no longer be contained within the permafrost by 2100 (or beyond). Hence this carbon is subject to increased respiration (again see Figure 1 in Burke et al., 2017a), decomposition and loss to the atmosphere. As might be broadly expected, the loss of carbon from within the original permafrost generally follows the decline of permafrost itself. In these scenarios this corresponds to slow loss during the 20th century, faster loss during the 21st century, slower losses during the 22nd century and approximate stabilization by 2500. Figure 1c and d shows that for a stabilisation target of 2 °C there is between 225 and 345 Gt C (10th to 90th percentile) that is in the permafrost in year 1900, which will no longer be held in permafrost by year 2500. If the stabilization target is reduced to 1.5 °C, then ~60 to 100 Gt of this carbon would instead remain relatively inert, still contained

within the permanently frozen soil. Uncertainties in the amount of permafrost carbon lost at 2 °C stabilization arising from the differences between JULES-suppressR_{esp} and JULES-deepR_{esp} are similar to the differences between the 1.5 °C and 2 °C stabilization target. Comparing these simulations, 50 to 90 Gt (10^{th} to 90^{th} percentile) less permafrost carbon is lost from JULES-suppressR_{esp}.

Permafrost carbon feedback

Our modelling structure allows a quantification of the permafrost carbon cycle feedback by isolating the atmosphere from any decomposed permafrost carbon. In 2100, when the global mean temperatures are approaching stabilization, the ensemble median of the permafrost carbon feedback for JULES-suppressR_{esp} is 0.027 °C and 0.040 °C for JULES-deepR_{esp} (Supplementary Information, Figure 4). This feedback has only increased slightly with an ensemble median of 0.030 °C (JULES-suppressR_{esp}) and 0.045 °C (JULES-deepR_{esp}) by 2500 (Figure 2a). The maximum feedback is less than 0.1 °C. Figure 2a shows there is little sensitivity to the stabilization target with the curves for the 1.5 and 2 °C targets falling relatively close to each other. JULES-suppressR_{esp} has a systematically smaller feedback (by ~0.02 °C) than JULES-deepR_{esp} and the climate uncertainty introduces a spread of 0.03 °C in the feedback.

Figure 2b also shows that the permafrost carbon feedback is a notable percentage of the overall global mean temperature change with values up to 5 % for 2500. These percentages are very similar for 2100 (Supplementary Information, Figure 4). Also clearly visible in Figure 2b is the fact that the permafrost carbon has a larger percentage impact on the global mean temperature change for the 1.5 °C stabilization target than for the 2 °C stabilization target. For example, in the case of JULES-deepR_{esp} and a 1.5 °C stabilization target, the permafrost carbon feedback accounts for, on average, 3 % of the overall global mean temperature change. In JULES-suppressR_{esp} for the 2 °C stabilization target the permafrost carbon feedback has the smallest percentage impact of, on average, 1.5 % of the total.

Carbon budgets

The annual exchange of carbon for the permafrost enabled simulations (Supplementary information Figure 5) shows both the land and ocean uptake some of the anthropogenic emissions before the stabilization year. By definition, after the year of CO_2 stabilization, the net emissions are zero. Any anthropogenic emissions after the year of stabilization are taken up by either the land or the ocean. These emissions are said to be compatible emissions and in the current simulations they remain positive throughout the simulation. The annual ocean and land uptake reduce with increased time after stabilization. In all cases the ocean continues to uptake carbon throughout the simulations. However, in some of the ensemble members the land becomes a source of carbon and in some it is a sink of carbon (Figure 3). This annual exchange of global land carbon is broken down into components in Figure 3 for two different time periods 2100 and 2500. [Additionally Supplementary information, Figure 6 shows the land carbon exchange for the permafrost region defined by the soil frozen state in 1860]. There is a notable decline in the vegetation and soil carbon fluxes between 2100 and 2500. In the 2 °C stabilization scenario around 2100 the vegetation uptake is around 0.25 Gt C per year. This uptake is approximately equal to the loss of old permafrost carbon as suggested by Pugh et al. (2017). By 2500 the vegetation uptake is 60 % less (around 0.05 Gt C per year) - around half the loss of old carbon at that time. As might be expected the vegetation always uptakes less for the 1.5 °C scenario due to lower atmospheric CO_2.

In 2100 the total soil carbon typically increases (Figure 3a) suggesting that the increase in vegetation growth and litter fall outweighs the increase in respiration caused by increased soil temperature. However by 2500 the respiration in JULES-deepR_{esp} tends to outweigh the increase in litter fall and there is an overall loss of total soil carbon (Figure 3b). This is not the case for JULES-suppressR_{esp} - total soil carbon is still increasing for JULES-suppressR_{esp}. Adding the total soil and vegetation carbon uptake gives a global land uptake of between 0.1 and 1.4 Gt C per year in 2100. By 2500 the land uptake has reduced to a small fraction of its value in 2100. For 10 of the ensemble members, the land has changed from a sink to a source of carbon. In 2500 when the climate is stable the land ranges from a sink of 0.12 to a source of 0.26 Gt C per year.

The impact of the old soil carbon that was in the pre-industrial permafrost on the global carbon budgets was identified. [By definition, the old carbon can only decrease.] Old carbon emissions are between 0.10 and 0.26 Gt C per year in 2100 (10^{th} to 90^{th} percentile, denoted PFC in Figure 3a) and- reduce the land carbon uptake. PFC emissions are only slightly less in 2500 - 0.08 to 0.18 Gt C per year (10^{th} to 90^{th} percentile). In 2500, when there are lower land carbon exchanges, these old emissions contribute in magnitude more than the vegetation to the global carbon fluxes and are the reason the land changes from a sink to a source of carbon in some cases. The loss of old permafrost carbon to the atmosphere is highly dependent on the parameterisation of the soil respiration – annually JULES-deepR_{esp} emits over twice as much PFC as JULES-suppressR_{esp}. The differences in PFC emissions between the two versions of JULES outweigh any small differences between the two stabilization targets and the minor impact of uncertainties in the climate response (Figure 3b).

Discussion and Conclusions

A coupled climate modelling system of intermediate complexity (including vegetation dynamics) is used to quantify the impact of permafrost carbon release on our ability to stabilise climate at 1.5 and 2 °C global mean temperature change by the year 2500. Simulations project that including permafrost carbon effects results in an additional temperature increase of 0.025 to 0.062 °C in the year 2500 (10^{th} to 90^{th} percentile). This is equivalent to between 1.5 and 3.8 % (10^{th} to 90^{th} percentile) of the final global mean temperature change at stabilization. A range of uncertainties including the stabilization target (policy uncertainty), climate response (spread across driving GCMs), and parameterisation of the soil carbon decomposition (process uncertainty) are sampled. It is found that the climate response and process uncertainty dominates over the differences between policy targets. In future work these processes uncertainties need to be further constrained by utilizing, for example, observations of the depth dependence of the soil carbon residence time (He et al., 2016).

Under the proposed stabilization targets, up to 3 million km^2 of permafrost is lost. This falls to the lower end of the range of previous model based estimates (Koven et al., 2013; Slater et al. 2013). Recently, Chadburn et al. (2017) used an observational based constraint on permafrost loss to demonstrate the sensitivity of permafrost area loss to global mean warming at stabilization is between 2.9 and 5.0 million $km^2\ °C^{-1}$. This constrained estimate is larger than

the sensitivity of permafrost extent to temperature change found previously and in this paper. If our simulations underestimate the physical loss of permafrost, they are likely to also underestimate the amount of carbon vulnerable to decomposition.

Any of the extra 170 to 325 Gt C (10^{th} to 90^{th} percentile) that is no longer in the permafrost will not immediately be released but could over time respire back to the atmosphere. By 2100 we suggest that 22 to 41 Gt C (10^{th} to 90^{th} percentile) has been lost. Schuur et al. (2015), basing their work on available model simulations within the literature, suggested that on average 90 Gt C permafrost carbon will be released by 2100 under high emissions scenarios. In more recent work, Burke et al. (2017b) estimated less than half that amount. Burke et al. (2017b) also suggested that before 2100 the amount of permafrost carbon emitted is relatively independent of the future emissions scenario.

JULES simulates a gradual loss of permafrost carbon as CO_2 in response to the increase in maximum thaw depth related to the temperature. In reality there will also be abrupt changes in the permafrost, for example when ground ice melts and parts of the landscape collapse (Jorgenson et al., 2006; Schädel et al., 2016). These thermokarst processes will result in increased soil carbon decomposition plus a change in the hydrology which might increase the proportion of carbon released in the form of methane (CH_4). Schädel et al. (2016) suggested any loss of CH_4 is still likely to be a small component of the permafrost carbon feedback. Additional processes within JULES that require refinements include soil carbon vertical mixing processes; the partitioning of organic matter into different lability pools along with their turnover times; and the dependence of decomposition on moisture and temperature. All of these effects are likely to modulate our estimate of permafrost thaw on both the global and arctic carbon cycle (Schuur et al., 2015).

Our overall finding is that including permafrost carbon in simulations of the global carbon budgets under 1.5 and 2 °C stabilization scenarios suggest that in 2100 an additional carbon uptake of 0.10 and 0.26 Gt C per year (10^{th} to 90^{th} percentile) is required. In addition a long-term carbon uptake of between 0.08 and 0.18 Gt C per year (10^{th} to 90^{th} percentile) is needed to maintain stabilization. A large majority of 1.5 or 2 °C pathways require substantial deployment of negative emission technology (NETs; Jones et al., 2016; Smith et al., 2015), and our findings

imply this will need to be larger than hereto projected. Using Bioenergy Carbon Capture and Storage (BECCS) to offset our modelled old soil carbon emissions in 2100 would require on average an additional 0.11 and 0.33 million km^2 of land, 21 to 65 km^3 per year of water for irrigation and costs between 3 and 10 billion $ per year (Smith et al., 2015).

Acknowledgements

The authors acknowledge funding and support from the Permafrost in the Arctic and Global Effects in the 21st century (PAGE21) Framework 7 project GA282700. E.J.B. and C.D.J were supported by the Joint UK DECC/Defra Met Office Hadley Centre Climate Programme (GA01101) and CRESCENDO (EU project 641816). Chris Huntingford acknowledges the NERC CEH Science Budget. S.E.C. is grateful to the University of Exeter for access to facilities and was supported by the Joint Partnership Initiative project COnstraining Uncertainties in the Permafrost-climate feedback (COUP) (National Environment Research Council grant NE/M01990X/1).

References

Best, M.J., Pryor, M., Clark, D.B., Rooney, G.G., Essery, R., Ménard, C.B., Edwards, J.M., Hendry, M.A., Porson, A., Gedney, N. and Mercado, L.M., 2011. The Joint UK Land Environment Simulator (JULES), model description–Part 1: energy and water fluxes. *Geoscientific Model Development*, *4*(3), pp.677-699.

Brown, J., O.J. Ferrians, Jr., J.A. Heginbottom, and E.S. Melnikov. 1998, revised February 2001. *Circum-arctic map of permafrost and ground ice conditions.* Boulder, CO: National Snow and Ice Data Center. Digital media.

Burke, E.J., Chadburn, S.E. and Ekici, A., 2017a. A vertical representation of soil carbon in the JULES land surface scheme (vn4. 3_permafrost) with a focus on permafrost regions. *Geoscientific Model Development*, *10*(2), p.959.

Burke, E.J., Ekici, A., Huang, Y., Chadburn, S.E., Huntingford, C., Ciais, P., Friedlingstein, P., Peng, S. and Krinner, G., 2017b. Quantifying uncertainties of permafrost carbon–climate feedbacks. *Biogeosciences*, *14*(12), p.3051.

Burke, E.J., Hartley, I.P. and Jones, C.D., 2012. Uncertainties in the global temperature change caused by carbon release from permafrost thawing. *The Cryosphere*, *6*(5), pp.1063-1076.

Burke, E.J., Jones, C.D. and Koven, C.D., 2013. Estimating the permafrost-carbon climate response in the CMIP5 climate models using a simplified approach. *Journal of Climate*, *26*(14), pp.4897-4909.

Chadburn, S. E., Burke, E. J., Essery, R. L. H., Boike, J., Langer, M., Heikenfeld, M., Cox, P. M., and Friedlingstein, P.: Impact of model developments on present and future simulations of permafrost in a global land-surface model, The Cryosphere, 9, 1505-1521, doi:10.5194/tc-9-1505-2015, 2015b.

Chadburn, S., Burke, E., Essery, R., Boike, J., Langer, M., Heikenfeld, M.,Cox, P., and Friedlingstein, P.: An improved representation of physical permafrost dynamics in the JULES land-surface model, Geosci. Model Dev., 8, 1493-1508, doi:10.5194/gmd-8-1493-2015, 2015a.

Chadburn, S.E., Burke, E.J., Cox, P.M., Friedlingstein, P., Hugelius, G. and Westermann, S., 2017. An observation-based constraint on permafrost loss as a function of global warming. *Nature Climate Change*, *7*(5), pp.340-344.

Clark, D.B., Mercado, L.M., Sitch, S., Jones, C.D., Gedney, N., Best, M.J., Pryor, M., Rooney, G.G., Essery, R.L.H., Blyth, E. and Boucher, O., 2011. The Joint UK Land Environment Simulator (JULES), model description–Part 2: carbon fluxes and vegetation dynamics. *Geoscientific Model Development*, *4*(3), pp.701-722.

González-Eguino, M., and M. B. Neumann (2016), Significant implications of permafrost thawing for climate change control, Clim. Change, 136(2), 381–388, doi:10.1007/s10584-016-1666-5.

He, Y., Trumbore, S.E., Torn, M.S., Harden, J.W., Vaughn, L.J., Allison, S.D. and Randerson, J.T., 2016. Radiocarbon constraints imply reduced carbon uptake by soils during the 21st century. Science, 353(6306), pp.1419-1424.

Hugelius, G., Strauss, J., Zubrzycki, S., Harden, J. W., Schuur, E. A. G., Ping, C.L., Schirrmeister, L., Grosse, G., Michaelson, G. J., Koven, C. D., O'Donnell, J. A., Elberling, B., Mishra, U., Camill, P., Yu, Z., Palmtag, J., and Kuhry, P.: Estimated stocks of circumpolar permafrost carbon with quantified uncertainty ranges and identified data gaps, Biogeosciences, 11, 6573–6593, doi:10.5194/bg-11-6573-2014, 2014.

Huntingford, C and Cox, P.M.: An analogue model to derive additional climate change scenarios from existing GCM simulations, Climate Dynamics, 16, 575-586, 2000.

Huntingford, C., Harris, P. P., Gedney, N., Cox, P. M., Betts, R. A., Marengo, J. A., and Gash, J. H. C.: Using a GCM analogue model to investigate the potential for Amazonian forest dieback, Theor. Appl. Climatol., 78, 177–185, 2004.

IPCC, 2013: *Climate Change 2013: The Physical Science Basis. Contribution of Working Group I to the Fifth Assessment Report of the Intergovernmental Panel on Climate Change* [Stocker, T.F., D. Qin, G.-K. Plattner, M. Tignor, S.K. Allen, J. Boschung, A. Nauels, Y. Xia, V. Bex and P.M. Midgley (eds.)]. Cambridge University Press, Cambridge, United Kingdom and New York, NY, USA, 1535 pp, doi:10.1017/CBO9781107415324.

Jones, C., Robertson, E., Arora, V., Friedlingstein, P., Shevliakova, E., Bopp, L., Brovkin, V., Hajima, T., Kato, E., Kawamiya, M. and Liddicoat, S., 2013. Twenty-first-century compatible CO2 emissions and airborne fraction simulated by CMIP5 earth system models under four representative concentration pathways. Journal of Climate, 26(13), pp.4398-4413.

Jones, C.D., Ciais, P., Davis, S.J., Friedlingstein, P., Gasser, T., Peters, G.P., Rogelj, J., van Vuuren, D.P., Canadell, J.G., Cowie, A. and Jackson, R.B., 2016. Simulating the Earth system response to negative emissions. *Environmental Research Letters*, *11*(9), p.095012.

Jorgenson, M. T., Y. L. Shur, and E. R. Pullman (2006), Abrupt increase in permafrost degradation in Arctic Alaska, Geophys. Res. Lett., 33(2), L02503, doi:10.1029/2005GL024960.

Koven, C.D., Riley, W.J. and Stern, A., 2013. Analysis of permafrost thermal dynamics and response to climate change in the CMIP5 Earth System Models. Journal of Climate, 26(6), pp.1877-1900.

MacDougall, A.H., Avis, C.A. and Weaver, A.J., 2012. Significant contribution to climate warming from the permafrost carbon feedback. *Nature Geoscience*, *5*(10), pp.719-721.

Moss, R.H., Edmonds, J.A., Hibbard, K.A., Manning, M.R., Rose, S.K., Van Vuuren, D.P., Carter, T.R., Emori, S., Kainuma, M., Kram, T. and Meehl, G.A., 2010. The next generation of scenarios for climate change research and assessment. *Nature*, *463*(7282), pp.747-756.

Pugh T. A. M. , Jones C. D., Huntingford C., Burton C., Arneth A., Brovkin V., Lomas M., Robertson E., Piao S. and S. Sitch, 2017, A large committed long term sink of carbon due to vegetation dynamics, submitted to Earth's Future.

Rogelj, J., Den Elzen, M., Höhne, N., Fransen, T., Fekete, H., Winkler, H., Schaeffer, R., Sha, F., Riahi, K. and Meinshausen, M., 2016. Paris Agreement climate proposals need a boost to keep warming well below 2 C. *Nature*, *534*(7609), pp.631-639.

Schädel, C., Bader, M.K.F., Schuur, E.A., Biasi, C., Bracho, R., Čapek, P., De Baets, S., Diáková, K., Ernakovich, J., Estop-Aragones, C. and Graham, D.E., 2016. Potential carbon emissions dominated by carbon dioxide from thawed permafrost soils. *Nature Climate Change*, *6*(10), pp.950-953.

Schleussner, C.F., Rogelj, J., Schaeffer, M., Lissner, T., Licker, R., Fischer, E.M., Knutti, R., Levermann, A., Frieler, K. and Hare, W., (2016). Science and policy characteristics of the Paris Agreement temperature goal. *Nature Climate Change*., 6, 827-835, doi:10.1038/nclimate3096.

Schneider von Deimling, T., Grosse, G., Strauss, J., Schirrmeister, L., Morgenstern, A., Schaphoff, S., Meinshausen, M. and Boike, J., 2015. Observation-based modelling of permafrost carbon fluxes with accounting for deep carbon deposits and thermokarst activity. *Biogeosciences*, *12*(11), pp.3469-3488.

Schuur, E.A.G., McGuire, A.D., Schädel, C., Grosse, G., Harden, J.W., Hayes, D.J., Hugelius, G., Koven, C.D., Kuhry, P., Lawrence, D.M. and Natali, S.M., 2015. Climate change and the permafrost carbon feedback. *Nature*, *520*(7546), pp.171-179.

Slater, A.G. and Lawrence, D.M., 2013. Diagnosing present and future permafrost from climate models. Journal of Climate, 26(15), pp.5608-5623.

Smith, P., Davis, S.J., Creutzig, F., Fuss, S., Minx, J., Gabrielle, B., Kato, E., Jackson, R.B., Cowie, A., Kriegler, E. and Van Vuuren, D.P., 2016. Biophysical and economic limits to negative CO2 emissions. *Nature Climate Change*, *6*(1), pp.42-50.

Weedon, G.P., Gomes, S., Viterbo, P., Shuttleworth, W.J., Blyth, E., Österle, H., Adam, J.C., Bellouin, N., Boucher, O. and Best, M., 2011. Creation of the WATCH forcing data and its use to assess global and regional reference crop evaporation over land during the twentieth century. Journal of Hydrometeorology, 12(5), pp.823-848.

Zelazowski, P., Huntingford, C., Mercado, L. M., and Schaller, N.: Climate pattern scaling set for an ensemble of 22 GCMs – adding uncertainty to the IMOGEN impacts system, Geosci. Model Dev. Discuss., https://doi.org/10.5194/gmd-2016-221, in review, 2016.

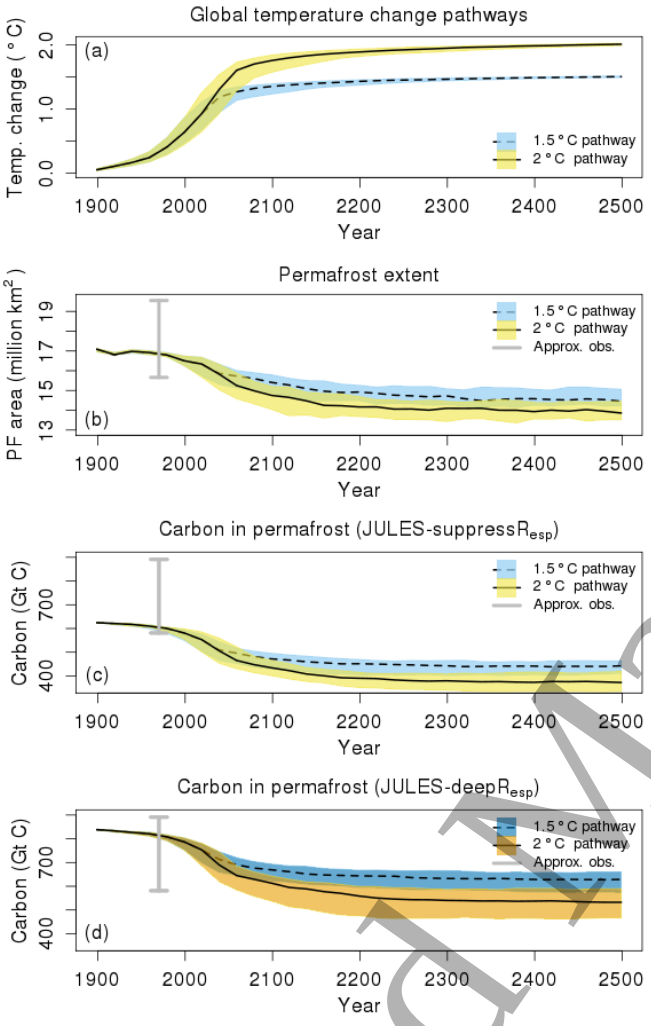

Figure 1 – Global mean temperature change, permafrost extent and permafrost carbon content. The time series of **(a)** global mean temperature change for the 1.5 and 2 °C pathways and **(b)** permafrost extent, both for JULES-suppressR$_{esp}$. There are no feedbacks within JULES from the soil carbon cycle onto the model physics so the time series for JULES-deepR$_{esp}$ are very similar and not shown. The time series of soil carbon still retained within the permafrost at each time are presented for the two configurations **(c)** JULES-suppressR$_{esp}$ and **(d)** JULES-deepR$_{esp}$. The 10th to 90th percentile range of the uncertainties in the response is shown, based on the spread of GCMs emulated. The ensemble mean is the black line, towards the middle of each spread (dashed for the 1.5 °C pathway and solid for the 2 °C pathway). The grey lines in (b), (c) and (d) represent an estimate of the equivalent observed value.

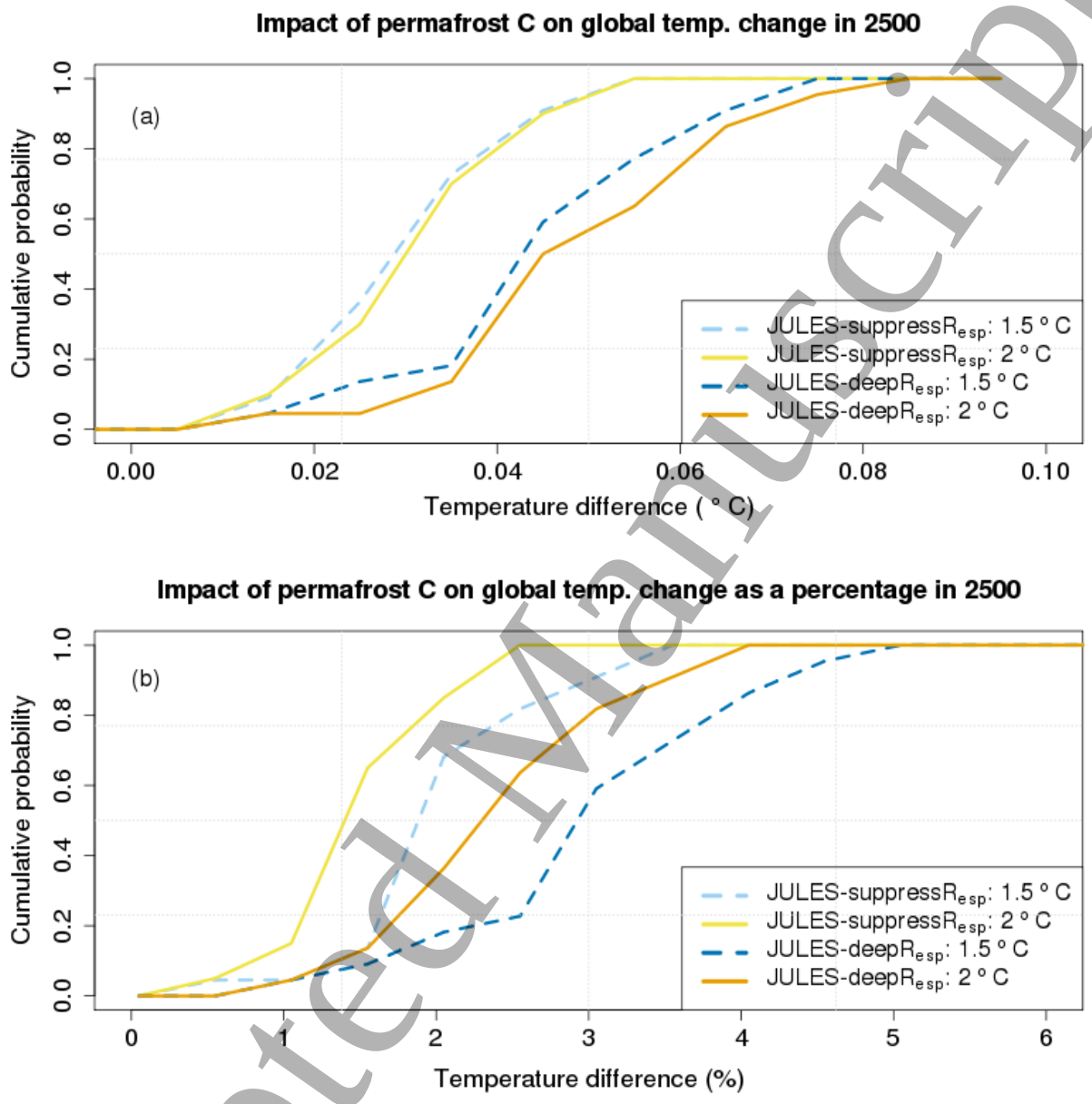

Figure 2. Permafrost thaw impact on global temperatures. The cumulative distribution of the impact of the old permafrost carbon release on the change in global air temperature in 2500. These show the fraction of the ensemble members with a feedback less than the value shown on the x-axis**. (a)** shows the impact in extra warming (°C) and **(b)** shows the impact as a percentage of the final stabilization temperature.

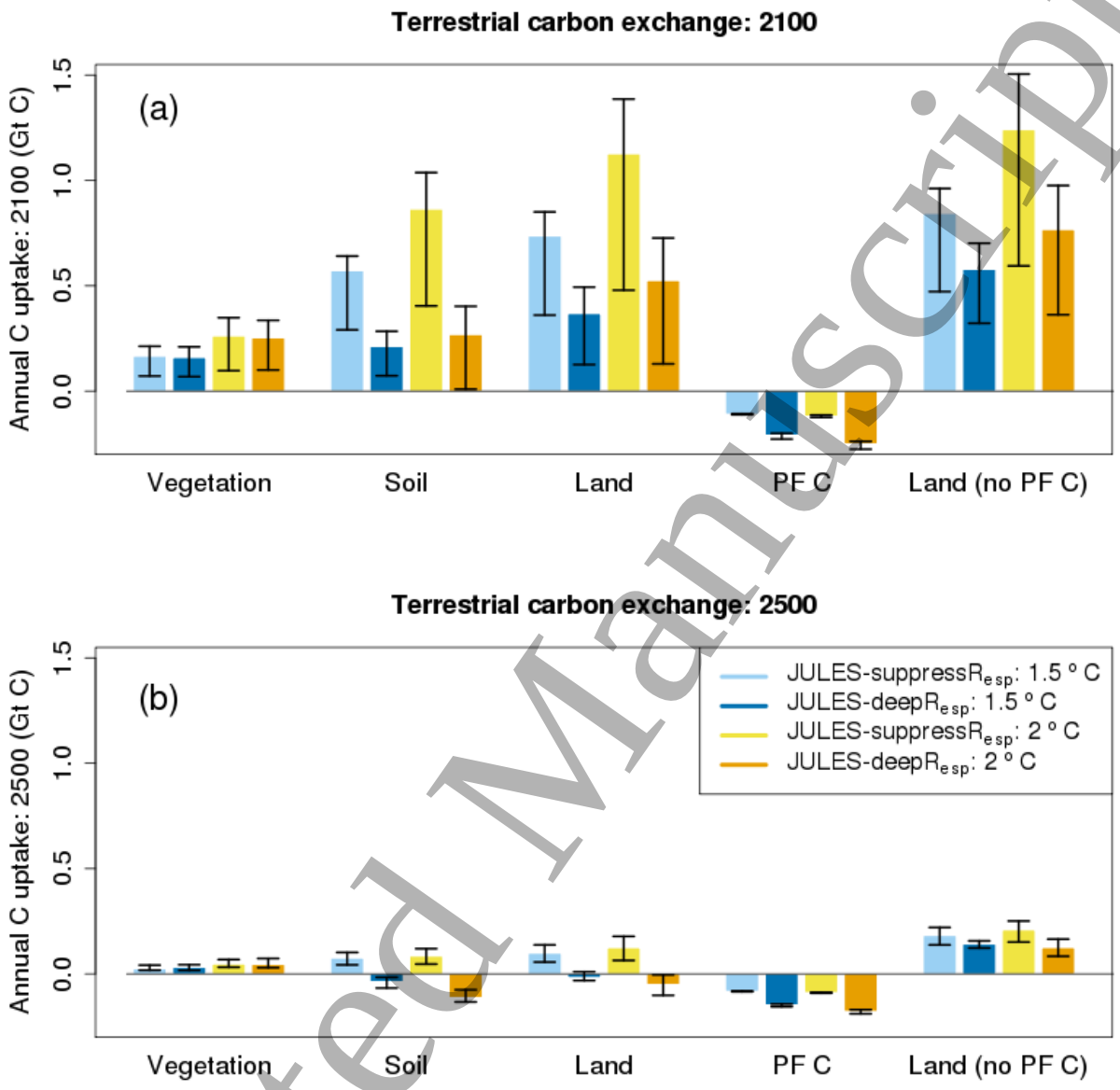

508 **Figure 3. Terrestrial global carbon exchanges**. Predicted annual global carbon exchange for
509 the components of the land carbon balance, at two future dates of 2100 and 2500. Shown are
510 the land (soil + vegetation) carbon, vegetation carbon and the total soil carbon from which the
511 old permafrost carbon can be separated. The error bars represent 25th to 75th percentile spread.
512 **(a)** is for the year 2100 and **(b)** for 2500. The vertical scales are kept identical to allow
513 comparison.
514